

A novel integral equation for scattering by locally rough surfaces and application to the inverse problem

Haiwen Zhang, Bo Zhang
 LSEC and Institute of Applied Mathematics
 Academy of Mathematics and Systems Science
 Chinese Academy of Sciences
 Beijing 100190, China
 (zhanghaiwen@amss.ac.cn, b.zhang@amt.ac.cn)

Abstract

This paper is concerned with the direct and inverse acoustic or electromagnetic scattering problems by a locally perturbed, perfectly reflecting, infinite plane (which is called a locally rough surface in this paper). We propose a novel integral equation formulation for the direct scattering problem which is defined on a bounded curve (consisting of a bounded part of the infinite plane containing the local perturbation and the lower part of a circle) with two corners. This novel integral equation can be solved efficiently by using the Nyström method with a graded mesh introduced previously by Kress and is capable of dealing with large wavenumber cases. For the inverse problem, we propose a Newton iteration method to reconstruct the local perturbation of the plane from multiple frequency far-field data, based on the novel integral equation formulation. Numerical examples are carried out to demonstrate that our reconstruction method is stable and accurate even for the case of multiple-scale profiles.

Keywords: Integral equation, locally rough surface, inverse scattering problem, far field pattern, perfectly reflecting surface, Newton iteration.

1 Introduction

Consider problems of scattering of plane acoustic or electromagnetic waves by a locally perturbed, perfectly reflecting, infinite plane (which is called a locally rough surface). Such problems occur in many applications such as radar, remote sensing, geophysics, medical imaging and nondestructive testing (see, e.g. [2, 4, 7, 8, 19]).

In this paper we restrict the discussion to the two-dimensional case by assuming that the local perturbation is invariant in the x_3 direction. We assume throughout that the incident wave is time-harmonic ($e^{-i\omega t}$ time dependence), so that the total wave field u satisfies the Helmholtz equation

$$\Delta u + k^2 u = 0 \quad \text{in } D_+. \quad (1.1)$$

Here, $D_+ := \{(x_1, x_2) \mid x_2 > h_\Gamma(x_1), x_1 \in \mathbb{R}\}$ represents a homogeneous medium above the locally rough surface denoted by $\Gamma := \partial D_+ = \{(x_1, x_2) \mid x_2 = h_\Gamma(x_1), x_1 \in \mathbb{R}\}$ with some smooth function $h_\Gamma \in C^2(\mathbb{R})$

having a compact support in \mathbb{R} , $k = \omega/c > 0$ is the wave number, ω and c are the frequency and speed of the wave in D_+ , respectively. Throughout, we will assume that the incident field u^i is the plane wave

$$u^i(x) = \exp(ikd \cdot x),$$

where $d = (\sin \theta, -\cos \theta) \in S_-$ is the incident direction, θ is the angle of incidence, measured from the x_2 -axis with $-\pi/2 < \theta < \pi/2$, and $S_- := \{x = (x_1, x_2) \mid |x| = 1, x_2 < 0\}$ is the lower part of the unit circle $S = \{x \in \mathbb{R}^2 \mid |x| = 1\}$. We further assume that the total field $u(x) = u^i(x) + u^r(x) + u^s(x)$ vanishes on the surface Γ :

$$u(x) = u^i(x) + u^r(x) + u^s(x) = 0 \quad \text{on } \Gamma, \quad (1.2)$$

where u^r is the reflected wave by the infinite plane $x_2 = 0$:

$$u^r(x) = -\exp(ik[x_1 \sin \theta + x_2 \cos \theta])$$

and u^s is the unknown scattered wave to be determined which is required to satisfy the Sommerfeld radiation condition

$$\lim_{r \rightarrow \infty} r^{\frac{1}{2}} \left(\frac{\partial u^s}{\partial r} - ik u^s \right) = 0, \quad r = |x|, \quad x \in D_+. \quad (1.3)$$

This problem models scattering of electromagnetic plane waves by a locally perturbed, perfectly conducting, infinite plane in the TE polarization case; it also models acoustic scattering by a one-dimensional sound-soft surface. Figure 1 presents the problem geometry.

The well-posedness of the scattering problem (1.1)-(1.3) has been studied by using the variational method with a Dirichlet-to-Neumann (DtN) map in [4] or the integral equation method in [30]. In particular, it was proved in [30] that u^s has the following asymptotic behavior at infinity:

$$u^s(x) = \frac{e^{ik|x|}}{\sqrt{|x|}} \left(u^\infty(\hat{x}; d) + O\left(\frac{1}{|x|}\right) \right), \quad |x| \rightarrow \infty$$

uniformly for all observation directions $\hat{x} \in S_+$ with $S_+ := \{x = (x_1, x_2) \mid |x| = 1, x_2 > 0\}$ the upper part of the unit circle S , where $u^\infty(\hat{x}; d)$ is called the far field pattern of the scattered field u^s , depending on the observation direction \hat{x} and the incident direction $d \in S_-$. The integral equation formulation obtained in [30] is of the second kind with a compact integral operator defined on the local perturbation part of the infinite plane. However, it is not suitable for numerical computation since it also involves an infinite integral over the unbounded, unperturbed part of the infinite plane. In [4], the scattering problem (1.1)-(1.3) is reformulated as an equivalent boundary value problem in a bounded domain with a DtN map on the part in D_+ of a large circle enclosing the local perturbation of the plane. This equivalent boundary value problem with a non-local boundary condition is then solved numerically by using the integral equation approach. However, the integral equation thus obtained involves a non-local DtN map on the semi-circle which needs to be truncated in numerical computations.

In this paper, we propose a novel integral equation formulation for the scattering problem (1.1)-(1.3), which is defined on a bounded curve (consisting of a bounded part of the infinite plane containing the local perturbation and the lower part of a circle) with two corners. Compared with [4] and [30], our integral equation formulation does not involve any infinite integral or a DtN map and therefore leads to fast numerical solution of the scattering problem including the large wavenumber cases. In fact, our integral equation can be solved efficiently by using the Nyström method with a graded mesh at the two

corners introduced previously by Kress [24] (see Section 3 below). Furthermore, we are also interested in the *inverse problem* of determining the locally rough surface from the far field pattern $u^\infty(\hat{x}, d)$ for all $\hat{x} \in S_+$, $d \in S_-$. A Newton iteration method is presented to reconstruct the locally rough surface from multi-frequency far field data, and our novel integral equation is applied to solve the direct scattering problem in each iteration. From the numerical examples it is seen that multi-frequency data are necessary in order to get a stable and accurate reconstruction of the locally rough surface.

The mathematical and computational aspects of the scattering problem (1.1)-(1.3) have been studied extensively in the case when the local perturbation is below the infinite plane which is called the cavity problem (see, e.g. [1, 2, 6] and the references quoted there) and for the case of non-local perturbations which is called the rough surface scattering (see, e.g. [8, 9, 10, 11, 12, 13, 31]).

There are many works concerning numerical solutions of the inverse problem of reconstructing the rough surfaces from the scattered field data. For example, a Newton method was proposed in [27] to reconstruct a local rough surface from the far-field pattern under the condition that the local perturbation is both star-like and *over* the infinite plane. An optimization method was introduced in [3] to recover a mild, local rough surface from the scattered field measured on a straight line within one wavelength above the local rough surface, under the assumption that the local perturbation is *over* the infinite plane. In [4], a continuation approach over the wave frequency was developed for reconstructing a general, local rough surface from the scattered field measured on an upper half-circle enclosing the local perturbation, based on the choice of the descent vector field. The reconstruction obtained in [4] is stable and accurate due to the use of multi-frequency near-field data (see also [5]). It should be pointed out that the reconstruction algorithm developed in [4] does not work with multi-frequency far-field data. Note that our novel integral equation formulation can also be used to develop a similar Newton inversion algorithm with multiple frequency near-field data. For the numerical recovery of non-local rough surfaces we refer to [7, 14, 15, 19, 20]. For the inverse cavity problem, the reader is referred to [2, 21, 28].

This paper is organized as follows. In Section 2, a novel integral equation formulation is proposed to solve the direct scattering problem. Section 3 is devoted to the numerical solution of the novel integral equation. In Section 4, it is proved that the local rough surface can be uniquely determined by the far-field pattern corresponding to a countably infinite number of incident plane waves. The Frechet differentiability is also shown of the far-field operator which maps the surface profile function h_Γ to the corresponding far field pattern $u_k^\infty(\hat{x}, d)$. The Newton method with multi-frequency far-field data is given in Section 5, based on the novel integral equation solver in Section 3. In Section 6, numerical examples are carried out to demonstrate that our reconstruction algorithm is stable and accurate even for the case of multiple-scale profiles, which is similar to the inversion algorithm with multi-frequency near-field data developed in [4].

2 A novel integral equation formulation for the direct problem

Let $f = -(u^i + u^r)$. Then f is continuous on Γ and $f = 0$ on $\Gamma_0 := \{(x_1, x_2) \in \Gamma \mid x_2 = 0\}$, that is, f has a compact support on Γ . The scattering problem (1.1)-(1.3) can be reformulated as the Dirichlet problem (DP) in the following way:

Find $u^s \in C^2(D_+) \cap C(\overline{D_+})$ satisfying the Helmholtz equation (1.1) in D_+ , the Sommerfeld radiation condition (1.3) and the Dirichlet boundary condition:

$$u^s = f \quad \text{on } \Gamma. \quad (2.1)$$

The following uniqueness result has been proved in [30, Theorem 3.1] for the above Dirichlet problem (DP).

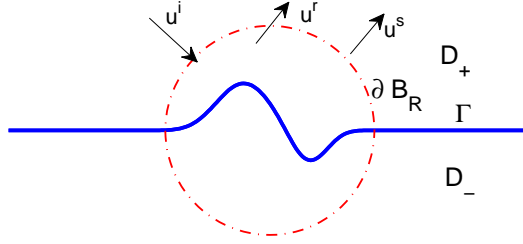


Figure 1: The scattering problem from a locally rough surface

Theorem 2.1. *The problem (DP) has at most one solution in $C^2(D_+) \cap C(\overline{D}_+)$.*

The existence of solutions to the problem (DP) has also been studied in [30] using an integral equation method. However, the integral equation obtained in [30] involves an infinite integral which yields difficulties in numerical computation. In this section, we propose a new integral equation to avoid this problem. To this end, we introduce the following notations. Let $B_R := \{x = (x_1, x_2) \mid |x| < R\}$ be a circle with $R > 0$ large enough so that the local perturbation $\Gamma_p := \Gamma \setminus \Gamma_0 = \{(x_1, h_\Gamma(x_1)) \mid x_1 \in \text{supp}(h_\Gamma)\} \subset B_R$. Then $\Gamma_R := \Gamma \cap B_R$ represents the part of Γ containing the local perturbation Γ_p of the infinite plane. Denote by $x_A := (-R, 0)$, $x_B := (R, 0)$ the endpoints of Γ_R . Write $\mathbb{R}_\pm^2 := \{(x_1, x_2) \in \mathbb{R}^2 \mid x_2 \gtrless 0\}$, $D_R^\pm := B_R \cap D_\pm$ and $\partial B_R^\pm := \partial B_R \cap D_\pm$, where $D_- := \{(x_1, x_2) \mid x_2 < h_\Gamma(x_1), x_1 \in \mathbb{R}\}$. See Figure 1.

For $\varphi \in C(\partial D_R^-)$ define S_k and \mathcal{D}_k to be the single- and double-layer potentials:

$$\begin{aligned} (S_k\varphi)(x) &:= \int_{\partial D_R^-} \Phi_k(x, y)\varphi(y)ds(y), \quad x \in \mathbb{R}^2 \setminus \partial D_R^- \\ (\mathcal{D}_k\varphi)(x) &:= \int_{\partial D_R^-} \frac{\partial \Phi_k(x, y)}{\partial \nu(y)} \varphi(y)ds(y), \quad x \in \mathbb{R}^2 \setminus \partial D_R^- \end{aligned}$$

and define $S_k, S_k^{re}, K_k, K_k^{re}$ to be the boundary integral operators of the following form:

$$\begin{aligned} (S_k\varphi)(x) &:= \int_{\partial D_R^-} \Phi_k(x, y)\varphi(y)ds(y), \quad x \in \partial D_R^- \\ (S_k^{re}\varphi)(x) &:= \begin{cases} \int_{\partial D_R^-} \Phi_k(x, y)\varphi(y)ds(y), & x \in \Gamma_R \\ \int_{\partial D_R^-} \Phi_k(x^{re}, y)\varphi(y)ds(y), & x \in \partial B_R^- \cup \{x_A, x_B\} \end{cases} \\ (K_k\varphi)(x) &:= \int_{\partial D_R^-} \frac{\partial \Phi_k(x, y)}{\partial \nu(y)} \varphi(y)ds(y), \quad x \in \partial D_R^- \\ (K_k^{re}\varphi)(x) &:= \begin{cases} \int_{\partial D_R^-} \frac{\partial \Phi_k(x, y)}{\partial \nu(y)} \varphi(y)ds(y), & x \in \Gamma_R \\ \int_{\partial D_R^-} \frac{\partial \Phi_k(x^{re}, y)}{\partial \nu(y)} \varphi(y)ds(y), & x \in \partial B_R^- \cup \{x_A, x_B\} \end{cases} \end{aligned}$$

where $x^{re} = (x_1, -x_2)$ is the reflection of $x = (x_1, x_2)$ about the x_1 -axis, $\Phi_k(x, y)$ is the fundamental solution of the Helmholtz equation $\Delta w + k^2 w = 0$ with the wavenumber k , and ν is the unit outward normal on ∂D_R^- . Note that $\Phi_0(x, y) = -1/(2\pi) \ln|x - y|$ is the fundamental solution of the Laplace equation.

Remark 2.2. Let $\varphi \in C(\partial D_R^-)$. From [22, Theorem 15.8b] it follows that the single-layer potential $S_k\varphi$ is continuous throughout \mathbb{R}^2 . In addition, from [26, Section 6.5] we know that the double-layer potential $\mathcal{D}_0\varphi$ can be continuously extended from $\mathbb{R}^2 \setminus \overline{D}_R$ to $\mathbb{R}^2 \setminus D_R^-$ with the limiting value

$$(\mathcal{D}_0\varphi)_+(x) = \begin{cases} (K_0\varphi)(x) + \frac{1}{2}\varphi(x) & \text{for } x \in \partial D_R^- \setminus \{x_A, x_B\} \\ (K_0\varphi)(x) + \frac{\gamma(x)}{2\pi}\varphi(x) & \text{for } x \in \{x_A, x_B\} \end{cases}$$

where $\gamma(x)$ is the interior angle at the corner $x \in \{x_A, x_B\}$. It remains valid for $\mathcal{D}_k\varphi$ with $k > 0$ since the kernel of $\mathcal{D}_k - \mathcal{D}_0$ is weakly singular which yields that $(\mathcal{D}_k - \mathcal{D}_0)\varphi$ is continuous throughout \mathbb{R}^2 . Thus from the jump relations, $S_k, S_k^{re}, \widetilde{K}_k$ and \widetilde{K}_k^{re} are bounded in $C(\partial D_R^-)$, where \widetilde{K}_k and \widetilde{K}_k^{re} are given by

$$\begin{aligned} (\widetilde{K}_k\varphi)(x) &:= \begin{cases} (K_k\varphi)(x) & \text{for } x \in \partial D_R^- \setminus \{x_A, x_B\} \\ (K_k\varphi)(x) + \left(\frac{\gamma(x)}{2\pi} - \frac{1}{2}\right)\varphi(x) & \text{for } x \in \{x_A, x_B\} \end{cases} \\ (\widetilde{K}_k^{re}\varphi)(x) &:= \begin{cases} (K_k^{re}\varphi)(x) & \text{for } x \in \partial D_R^- \setminus \{x_A, x_B\} \\ (K_k^{re}\varphi)(x) + \left(\frac{\gamma(x)}{2\pi} - \frac{1}{2}\right)\varphi(x) & \text{for } x \in \{x_A, x_B\} \end{cases} \end{aligned}$$

In particular, $S_k - S_0, S_k^{re} - S_0^{re}, \widetilde{K}_k - K_0$ and $\widetilde{K}_k^{re} - K_0^{re}$ are bounded in $C(\partial D_R^-)$.

Let u^s be the solution of the problem (DP). Then we can extend $u^s(x)$ into $\mathbb{R}^2 \setminus \overline{B}_R$ by reflection, which is denoted again by $u^s(x)$, such that $u^s(x) = -u^s(x^{re})$ in $\mathbb{R}^2 \setminus \overline{B}_R$. By a regularity argument (see [16, page 88] or [30, Theorem 3.1]) and the reflection principle, we know that $u^s \in C^2(\mathbb{R}^2 \setminus \overline{D}_R) \cap C(\mathbb{R}^2 \setminus D_R^-)$ and satisfies the Helmholtz equation (1.1) in $\mathbb{R}^2 \setminus \overline{D}_R$. Following the idea in [17], we seek the solution u^s in the form

$$u^s(x) = (\mathcal{D}_k\varphi)(x) - i\eta(S_k\varphi)(x), \quad \varphi \in C(\partial D_R^-), \quad x \in \mathbb{R}^2 \setminus \partial D_R^- \quad (2.2)$$

where $\eta \neq 0$ is a real coupling parameter. Let ψ^{re} be a continuous mapping from ∂D_R^- to ∂D_R^+ such that

$$\psi^{re}(x) = \begin{cases} x, & x \in \Gamma_R \\ x^{re}, & x \in \partial B_R^- \cup \{x_A, x_B\} \end{cases}$$

Since $u^s(x) + u^s(\psi^{re}(x)) = -2[u^i(x) + u^r(x)]$ on Γ_R and $u^s(x) + u^s(\psi^{re}(x)) = 0$ on $\partial B_R^- \cup \{x_A, x_B\}$, and by the jump relations of the layer potentials, we obtain the boundary integral equation $P\varphi(x) = g(x)$, where

$$P\varphi := \begin{cases} \varphi + (K_k\varphi - i\eta S_k\varphi) + (K_k^{re}\varphi - i\eta S_k^{re}\varphi), & x \in \Gamma_R \\ \frac{1}{2}\varphi + (K_k\varphi - i\eta S_k\varphi) + (K_k^{re}\varphi - i\eta S_k^{re}\varphi), & x \in \partial B_R^- \cup \{x_A, x_B\} \end{cases} \quad (2.3)$$

and

$$g(x) := \begin{cases} -2(u^i(x) + u^r(x)), & x \in \Gamma_R \\ 0, & x \in \partial B_R^- \cup \{x_A, x_B\} \end{cases} \quad (2.4)$$

Here, we have used the fact that the interior angles $\gamma(x)$ at the corners x_A, x_B are both $\pi/2$. Note that $g \in C(\partial D_R^-)$. Further, from Remark 2.2 and the continuity of ψ^{re} it follows that P is a bounded linear operator in $C(\partial D_R^-)$.

Conversely, we have the following result.

Lemma 2.3. Assume that u^s is of the form (2.2) with $\varphi \in C(\partial D_R^-)$ which satisfies the integral equation $P\varphi = g$ with P, g defined in (2.3), (2.4), respectively. Then $u^s \in C^2(D_+) \cap C(\overline{D}_+)$ and solves the problem (DP).

Proof. Since $\varphi \in C(\partial D_R^-)$, it follows from Remark 2.2 that $u^s \in C^2(\mathbb{R}^2 \setminus \overline{D}_R) \cap C(\mathbb{R}^2 \setminus D_R^-)$ and satisfies the Helmholtz equation (1.1) in $\mathbb{R}^2 \setminus \overline{D}_R$. In addition, $P\varphi = g$ implies that $u^s(x) + u^s(x^{re}) = 0$ on $\partial B_R^- \cup \{x_A, x_B\}$ and $u^s(x) = -(u^i(x) + u^r(x))$ on Γ_R .

Let $\tilde{u}^s(x) = -u^s(x^{re})$ in $\mathbb{R}^2 \setminus B_R$. Then \tilde{u}^s satisfies the Helmholtz equation (1.1) in $\mathbb{R}^2 \setminus \overline{B}_R$ and $\tilde{u}^s(x) = u^s(x)$ on ∂B_R . Moreover, the uniqueness of the exterior Dirichlet problem (see, e.g. [17, Chapter 3]) implies that $\tilde{u}^s = u^s$ in $\mathbb{R}^2 \setminus B_R$. In particular, $u^s(x) = 0$ on $\Gamma \setminus \Gamma_R$ which yields that $u^s(x) = -(u^i + u^r)$ on Γ . The proof is thus completed. \square

We now prove the unique solvability of the integral equation $P\varphi = g$.

Theorem 2.4. The integral equation $P\varphi = g$ has a unique solution $\varphi \in C(\partial D_R^-)$ satisfying the estimate

$$\|\varphi\|_{C(\partial D_R^-)} \leq C\|u^i + u^r\|_{C(\Gamma)} \quad (2.5)$$

Proof. We need to deal with the corners. Following the idea in [17], we introduce the following boundary integral operators: for $z = x_A, x_B$

$$K_{0,z}\varphi(x) := \int_{\partial D_R^-} \frac{\partial \Phi_0(x,y)}{\partial \nu(y)} \varphi(z) ds(y), \quad x \in \partial D_R^-$$

$$K_{0,z}^{re}\varphi(x) := \begin{cases} \int_{\partial D_R^-} \frac{\partial \Phi_0(x,y)}{\partial \nu(y)} \varphi(z) ds(y), & x \in \Gamma_R \\ \int_{\partial D_R^-} \frac{\partial \Phi_0(x^{re},y)}{\partial \nu(y)} \varphi(z) ds(y), & x \in \partial B_R^- \cup \{x_A, x_B\} \end{cases}$$

For $z = x_A, x_B$ define $B_\varepsilon(z) := \{x \in \mathbb{R}^2 \mid |x-z| < \varepsilon\}$ with radius ε small enough such that $B_\varepsilon(z) \cap (\Gamma \setminus \Gamma_0) = \emptyset$. Choose a cut-off function $\chi \in C_0^\infty(\mathbb{R}^2)$ satisfying that $0 \leq \chi \leq 1$, $\chi(x) = \chi(x^{re})$, $\chi = 1$ in $B_\varepsilon(x_A)$ and $\chi = 0$ in $B_\varepsilon(x_B)$. Since $K_{0,z}\varphi$ vanishes in $\mathbb{R}^2 \setminus \overline{D}_R$ for $z = x_A, x_B$, we can rewrite (2.2) in the following form:

$$u^s(x) = \chi(x) \left[\int_{\partial D_R^-} \left(\frac{\partial \Phi_k(x,y)}{\partial \nu(y)} - i\eta \Phi_k(x,y) \right) \varphi(y) ds(y) - \int_{\partial D_R^-} \frac{\partial \Phi_0(x,y)}{\partial \nu(y)} \varphi(x_A) ds(y) \right]$$

$$+ [1 - \chi(x)] \left[\int_{\partial D_R^-} \left(\frac{\partial \Phi_k(x,y)}{\partial \nu(y)} - i\eta \Phi_k(x,y) \right) \varphi(y) ds(y) - \int_{\partial D_R^-} \frac{\partial \Phi_0(x,y)}{\partial \nu(y)} \varphi(x_B) ds(y) \right], \quad x \in \mathbb{R}^2 \setminus \overline{D}_R$$

Accordingly, using the jump relations of the layer potentials and the fact that $\chi(x) = \chi(x^{re})$, we rewrite $P\varphi$, defined in (2.3), as $P\varphi = I_\chi\varphi + A\varphi + B\varphi$, where

$$(I_\chi\varphi)(x) := \begin{cases} \varphi(x), & x \in \Gamma_R \\ (1/2)[\varphi(x) + \chi\varphi(x_A) + (1-\chi)\varphi(x_B)], & x \in \partial B_R^- \cup \{x_A, x_B\} \end{cases}$$

$$(A\varphi)(x) := -\chi(x)\varphi(x_A) - [1 - \chi(x)]\varphi(x_B)$$

$$(B\varphi)(x) := \chi(x) (K_k\varphi - i\eta S_k\varphi - K_{0,x_A}\varphi)(x) + [1 - \chi(x)] (K_k\varphi - i\eta S_k\varphi - K_{0,x_B}\varphi)(x)$$

$$+ \chi(x) (K_k^{re}\varphi - i\eta S_k^{re}\varphi - K_{0,x_A}^{re}\varphi)(x) + [1 - \chi(x)] (K_k^{re}\varphi - i\eta S_k^{re}\varphi - K_{0,x_B}^{re}\varphi)(x)$$

Here, I_χ, A are bounded in $C(\partial D_R^-)$. From Remark 2.2, B is also bounded in $C(\partial D_R^-)$.

Step 1. We show that P is a Fredholm operator of index zero.

Let

$$(M_0\varphi)(x) := \chi(x)(K_0\varphi - K_{0,x_A}\varphi)(x) + [1 - \chi(x)](K_0\varphi - K_{0,x_B}\varphi)(x) \\ + \chi(x)(K_0^{re}\varphi - K_{0,x_A}^{re}\varphi)(x) + [1 - \chi(x)](K_0^{re}\varphi - K_{0,x_B}^{re}\varphi)(x)$$

From Remark 2.2 it is easy to see that M_0 is bounded in $C(\partial D_R^-)$. Since the integral operator $B - M_0$ has a weakly singular kernel and ψ^{re} is a continuous mapping, the operator $B - M_0$ is compact in $C(\partial D_R^-)$. Thus, $P - (I_\chi + M_0) = A + B - M_0$ is compact in $C(\partial D_R^-)$.

Moreover, for $z = x_A, x_B$ and $0 < r < \varepsilon$ choose a cut-off function $\psi_{r,z} \in C_0^\infty(\mathbb{R}^2)$ satisfying that $0 \leq \psi_{r,z} \leq 1$, $\psi_{r,z}(x) = 1$ in the region $0 \leq |x - z| \leq r/2$ and $\psi_{r,z}(x) = 0$ in the region $r \leq |x - z| < \infty$. Define $M_{0,r} : C(\partial D_R^-) \rightarrow C(\partial D_R^-)$ by

$$M_{0,r}\varphi := \psi_{r,x_A}\chi\left[K_0(\psi_{r,x_A}\varphi) - K_{0,x_A}(\psi_{r,x_A}\varphi(x_A))\right] \\ + \psi_{r,x_B}(1 - \chi)\left[K_0(\psi_{r,x_B}\varphi) - K_{0,x_B}(\psi_{r,x_B}\varphi(x_B))\right] \\ + \psi_{r,x_A}\chi\left[K_0^{re}(\psi_{r,x_A}\varphi) - K_{0,x_A}^{re}(\psi_{r,x_A}\varphi(x_A))\right] \\ + \psi_{r,x_B}(1 - \chi)\left[K_0^{re}(\psi_{r,x_B}\varphi) - K_{0,x_B}^{re}(\psi_{r,x_B}\varphi(x_B))\right], \quad \varphi \in C(\partial D_R^-).$$

Since the kernel of $M_{0,r} - M_0$ vanishes in a neighborhood of (x_A, x_A) and (x_B, x_B) , it is compact in $C(\partial D_R^-)$. Thus $P - (I_\chi + M_{0,r})$ is compact in $C(\partial D_R^-)$ since $P - (I_\chi + M_0)$ is compact in $C(\partial D_R^-)$.

We now introduce the following norm on $C(\partial D_R^-)$:

$$\|\varphi\|_{\infty,0} := \max \left\{ \max_{\Gamma_R} \left[|\chi(\varphi - \varphi(x_A))| + |(1 - \chi)(\varphi - \varphi(x_B))| + |\varphi(x_A)| + |\varphi(x_B)| \right], \right. \\ \left. \max_{\partial B_R^- \cup \{x_A, x_B\}} \left[\left| \frac{1}{2}\chi(\varphi - \varphi(x_A)) \right| + \left| \frac{1}{2}(1 - \chi)(\varphi - \varphi(x_B)) \right| + |\varphi(x_A)| + |\varphi(x_B)| \right] \right\}$$

which is equivalent to the maximum norm $\|\cdot\|_\infty$. It is easy to see that I_χ is a bijection from $C(\partial D_R^-)$ to $C(\partial D_R^-)$ with

$$I_\chi^{-1}\psi = \begin{cases} \psi, & x \in \Gamma_R \\ 2\psi - \chi\psi(x_A) - (1 - \chi)\psi(x_B), & x \in \partial B_R^- \cup \{x_A, x_B\} \end{cases}$$

and $\|I_\chi\varphi\|_\infty \leq \|\varphi\|_{\infty,0}$ for all $\varphi \in C(\partial D_R^-)$. Furthermore, choose a function $\phi_0 \in C(\partial D_R^-)$ such that $\phi_0 \geq 0$, $\phi_0(x_A) = \phi_0(x_B) = 0$ and ϕ_0 reaches its maximum on Γ_R . Then $\|I_\chi\phi_0\|_\infty = \|\phi_0\|_{\infty,0}$, which implies that $\|I_\chi\|_{C(\partial D_R^-, \|\cdot\|_{\infty,0}) \rightarrow C(\partial D_R^-, \|\cdot\|_\infty)} = 1$.

We now prove that $\|M_{0,r}\|_{C(\partial D_R^-, \|\cdot\|_{\infty,0}) \rightarrow C(\partial D_R^-, \|\cdot\|_\infty)} < 1$ for $r > 0$ small enough. For any $\varphi \in C(\partial D_R^-)$, $\text{supp}(M_{0,r}\varphi) \subset B_r(x_A) \cup B_r(x_B)$, so we only need to consider $(M_{0,r}\varphi)(x)$ for $x \in \partial D_R^- \cap (B_r(x_A) \cup B_r(x_B))$. Note first that for $x \in \partial D_R^- \cap B_r(x_A)$ we have

$$(M_{0,r}\varphi)(x) = \psi_{r,x_A}\left[K_0(\psi_{r,x_A}\varphi) - K_{0,x_A}(\psi_{r,x_A}\varphi(x_A))\right] \\ = \psi_{r,x_A}\left[K_0^{re}(\psi_{r,x_A}\varphi) - K_{0,x_A}^{re}(\psi_{r,x_A}\varphi(x_A))\right].$$

Then the required estimate can be obtained by following the idea in [17, Section 3.5], together with the inequality:

$$|\nu(y) \cdot (x - y)| \leq C|x - y|^2 \tag{2.6}$$

for $x \in \Gamma_R \cup \{x_A, x_B\}$, $y \in \Gamma_R$ or for $x \in \partial B_R$, $y \in \partial B_R^-$.

When $x = x_A$, using (2.6) we have

$$|(M_{0,r}\varphi)(x_A)| \leq Cr\|\varphi\|_{\infty,0}$$

When $x \in \Gamma_R \cap B_r(x_A)$, the integral $(M_{0,r}\varphi)(x)$ can be split up into two parts: the first one over $\Gamma_R \cap B_r(x_A)$ and the second one over $\partial B_R^- \cap B_r(x_A)$. The first part can be bounded with the upper bound $Cr\|\varphi\|_{\infty,0}$, estimated directly using (2.6). Noting that $\nu(y) \cdot (x - y)$ does not change its sign for $x \in \Gamma_R \cap B_r(x_A)$ and $y \in \partial B_R^- \cap B_r(x_A)$, we have that for $x \in \Gamma_R \cap B_r(x_A)$ the second part is bounded by

$$\begin{aligned} & 2 \left| \psi_{r,x_A}(x) \int_{\partial B_R^-} \left[\frac{\partial \Phi_0(x,y)}{\partial \nu(y)} \psi_{r,x_A}(y) (\varphi(y) - \varphi(x_A)) \right] ds(y) \right| \\ & \leq 2 \int_{\partial B_R^- \cap B_r(x_A)} \left| \frac{\partial \Phi_0(x,y)}{\partial \nu(y)} \right| ds(y) \|\varphi\|_{\infty,0} \\ & = 2 \left| \int_{\partial B_R^- \cap B_r(x_A)} \frac{\partial \Phi_0(x,y)}{\partial \nu(y)} ds(y) \right| \|\varphi\|_{\infty,0} \\ & = \frac{\alpha(x)}{\pi} \|\varphi\|_{\infty,0} \end{aligned}$$

where $\alpha(x)$ is the angle between the two segments connecting x and the two endpoints of the arc $\partial B_R^- \cap B_r(x_A)$. Since the interior angle at x_A is $\pi/2$, we have $\alpha(x) \leq 3\pi/4$ if r is small enough. Thus, for $x \in \Gamma_R \cap B_r(x_A)$ we have

$$|(M_{0,r}\varphi)(x)| \leq (Cr + 3/4)\|\varphi\|_{\infty,0}$$

When $x \in \partial B_R^- \cap B_r(x_A)$, the integral $(M_{0,r}\varphi)(x)$ can also be split up into two parts: the first one over $\Gamma_R \cap B_r(x_A)$ and the second one over $\partial B_R^- \cap B_r(x_A)$. Since $\partial \ln|x - y|/\partial \nu(y) = -x_2/|x - y|^2$ for $y \in \Gamma_R \cap B_r(x_A)$, then, for $x \in \partial B_R^- \cap B_r(x_A)$ the first part is equal to

$$\begin{aligned} & \psi_{r,x_A}(x) \int_{\Gamma_R} \left[\frac{\partial \Phi_0(x,y)}{\partial \nu(y)} \psi_{r,x_A}(y) (\varphi(y) - \varphi(x_A)) \right] ds(y) \\ & + \psi_{r,x_A}(x) \int_{\Gamma_R} \left[\frac{\partial \Phi_0(x^r e, y)}{\partial \nu(y)} \psi_{r,x_A}(y) (\varphi(y) - \varphi(x_A)) \right] ds(y) = 0, \end{aligned}$$

whilst the second part can be estimated using (2.6) and is bounded with the upper bound $Cr\|\varphi\|_{\infty,0}$. Thus, for $x \in \partial B_R^- \cap B_r(x_A)$ we have

$$|(M_{0,r}\varphi)(x)| \leq Cr\|\varphi\|_{\infty,0}$$

Similar estimates can be obtained for $(M_{0,r}\varphi)(x)$ when $x \in \partial D_R^- \cap B_r(x_B)$. Thus we have the estimate

$$|(M_{0,r}\varphi)(x)| \leq (Cr + 3/4)\|\varphi\|_{\infty,0}$$

for $x \in \partial D_R^- \cap (B_r(x_A) \cup B_r(x_B))$. Choosing $r > 0$ small enough we obtain that $\|M_{0,r}\|_{C(\partial D_R^-, \|\cdot\|_{\infty,0}) \rightarrow C(\partial D_R^-, \|\cdot\|_{\infty})} < 1$. Then, by the Neumann series, $I_\chi + M_{0,r}$ has a bounded inverse in $C(\partial D_R^-)$, yielding that P is a Fredholm operator of index zero since $P = [P - (I_\chi + M_{0,r})] + I_\chi + M_{0,r}$ and $P - (I_\chi + M_{0,r})$ is compact in $C(\partial D_R^-)$.

Step 2. We prove that P is injective and therefore invertible in $C(\partial D_R^-)$.

Let $P\varphi = 0$ for $\varphi \in C(\partial D_R^-)$. Then, by Lemma 2.3, the scattered field u^s defined by (2.2) vanishes on the boundary Γ . From Theorem 2.1 and Holmgren's uniqueness theorem, u^s vanishes in $\mathbb{R}^2 \setminus D_R^-$. On the other hand, by the jump relations of the layer potentials (see Remark 2.2), we have $(P_0\varphi)(x) = 0$ for $x \in \partial D_R^-$, where $(P_0\varphi)(x) := \alpha(x)\varphi(x) + (K_k\varphi)(x) - i\eta(S_k\varphi)(x)$ is bounded in $C(\partial D_R^-)$ with $\alpha(x) = 1/2$ for $x \in \partial D_R^- \setminus \{x_A, x_B\}$ and $\alpha(x) = \gamma(x)/(2\pi)$ for $x = x_A, x_B$. It was proved in [29] that P_0 has a bounded inverse in $C(\partial D_R^-)$, yielding that $\varphi = 0$.

By the Fredholm alternative, P is invertible with a bounded inverse P^{-1} in $C(\partial D_R^-)$. The proof is thus completed. \square

Combining Lemma 2.3, Theorems 2.1 and 2.4 and the mapping properties of the single- and double-layer potentials in the space of continuous functions, we get the following result on the well-posedness of the problem (DP).

Theorem 2.5. *The problem (DP) has a unique solution $u^s \in C^2(D_+) \cap C(\overline{D}_+)$. Furthermore,*

$$\|u^s\|_{C(\overline{D}_+)} \leq C\|u^i + u^r\|_{C(\Gamma)}. \quad (2.7)$$

Remark 2.6. By the asymptotic behavior of the fundamental solution Φ_k , we have the following far field pattern for the scattered field u^s given by (2.2):

$$u^\infty(\hat{x}) = \frac{e^{-i\pi/4}}{\sqrt{8\pi k}} \int_{\partial D_R^-} [k\nu(y) \cdot \hat{x} + \eta] e^{-ik\hat{x} \cdot y} \varphi(y) ds(y) \quad (2.8)$$

which is an analytic function on the unit circle S , where φ is the solution of the integral equation $P\varphi = g$.

3 Numerical solution of the novel integral equation

We make use of the Nyström method with a graded mesh introduced in [17, Section 3.5] (see also [24]) to solve the integral equation $P\varphi = g$. Let ∂D_R^- be parameterized as $x(s) = (x_1(s), x_2(s))$, $0 \leq s \leq 2\pi$ such that $(x_1(0), x_2(0)) = x_B$ and $(x_1(\pi), x_2(\pi)) = x_A$, where

$$\begin{aligned} x_1(s) &= \begin{cases} -2R\omega(s)/\pi + R, & 0 \leq s \leq \pi \\ R \cos(\omega(s)), & \pi < s \leq 2\pi \end{cases} \\ x_2(s) &= \begin{cases} h_\Gamma(-2R\omega(s)/\pi + R), & 0 \leq s \leq \pi \\ R \sin(\omega(s)), & \pi < s \leq 2\pi \end{cases} \end{aligned}$$

Here, $\omega : [0, 2\pi] \rightarrow [0, 2\pi]$ is a strictly, monotonically increasing function satisfying that $\omega(s) = \pi[v(s)]^p / ([v(s)]^p + [v(\pi - s)]^p)$ for $0 \leq s \leq \pi$ and $\omega(s) = \omega(s - \pi) + \pi$ for $\pi < s \leq 2\pi$, where

$$v(s) = \left(\frac{1}{p} - \frac{1}{2}\right) \left(\frac{\pi - 2s}{\pi}\right)^3 + \frac{1}{p} \cdot \frac{2s - \pi}{\pi} + \frac{1}{2}$$

with $p = 4$. Note that $\omega(0) = 0$, $\omega(\pi) = \pi$ and $\omega'(0) = \omega'(\pi) = 0$. Then the integral equation $P\varphi = g$ can be rewritten as $P\varphi(x(t)) = g(x(t))$, where

$$P\varphi(x(t)) = \begin{cases} \varphi(x(t)) + 2 \int_0^{2\pi} \left[\frac{\partial \Phi_k(x(t), x(s))}{\partial \nu(x(s))} - i\eta \Phi_k(x(t), x(s)) \right] |x'(s)| ds, & 0 < t < \pi \\ \frac{1}{2} \varphi(x(t)) + \int_0^{2\pi} \left[\frac{\partial \Phi_k(x(t), x(s))}{\partial \nu(x(s))} - i\eta \Phi_k(x(t), x(s)) \right] |x'(s)| ds \\ \quad + \int_0^{2\pi} \left[\frac{\partial \Phi_k(x^{re}(t), x(s))}{\partial \nu(x(s))} - i\eta \Phi_k(x^{re}(t), x(s)) \right] |x'(s)| ds, & \pi \leq t \leq 2\pi \end{cases}$$

For $j = 0, 1, \dots, 2n - 1$ with $n \in \mathbb{N}$ and $n > 0$, let $t_j = j\pi/n$ and $g_j = g(x(t_j))$. Then we get the approximation value $\varphi_j^{(n)}$ of φ at the points $x(t_j)$ by solving the linear system

$$\begin{aligned} \frac{1}{2}\varphi_i^{(n)} + 2 \sum_{j=1, j \neq n}^{2n-1} \left(R_{|i-j|}^{(n)} K_1(t_i, t_j) + \frac{\pi}{n} K_2(t_i, t_j) \right) \varphi_j^{(n)} &= g_i, & i = 0, n \\ \varphi_i^{(n)} + 2 \sum_{j=1, j \neq n}^{2n-1} \left(R_{|i-j|}^{(n)} K_1(t_i, t_j) + \frac{\pi}{n} K_2(t_i, t_j) \right) \varphi_j^{(n)} &= g_i, & i = 1, \dots, n-1 \\ \varphi_i^{(n)} + \sum_{j=1, j \neq n}^{2n-1} \left(R_{|i-j|}^{(n)} K_1(t_i, t_j) + \frac{\pi}{n} K_2(t_i, t_j) + \frac{\pi}{n} K_3(t_i, t_j) \right) \varphi_j^{(n)} &= g_i, & i = n+1, \dots, 2n-1 \end{aligned}$$

where, for $j = 0, 1, \dots, 2n - 1$

$$R_j^{(n)} := -\frac{2\pi}{n} \sum_{m=1}^{n-1} \frac{1}{m} \cos\left(\frac{mj\pi}{n}\right) - \frac{(-1)^j \pi}{n^2}$$

and for $i = 0, 1, \dots, 2n - 1$, $j = 1, 2, \dots, n - 1, n + 1, \dots, 2n - 1$

$$\begin{aligned} K(t_i, t_j) &:= \left[\frac{\partial \Phi_k(x(t_i), x(t_j))}{\partial v(x(t_j))} - i\eta \Phi_k(x(t_i), x(t_j)) \right] |x'(t_j)| \\ K_1(t_i, t_j) &:= -\frac{1}{4\pi} \left[\frac{\partial J_0(k|x(t_i) - x(t_j)|)}{\partial v(x(t_j))} - i\eta J_0(k|x(t_i) - x(t_j)|) \right] |x'(t_j)| \\ K_2(t_i, t_j) &:= K(t_i, t_j) - K_1(t_i, t_j) \ln\left(4 \sin^2 \frac{t_i - t_j}{2}\right) \\ K_3(t_i, t_j) &:= \left[\frac{\partial \Phi_k(x^{re}(t_i), x(t_j))}{\partial v(x(t_j))} - i\eta \Phi_k(x^{re}(t_i), x(t_j)) \right] |x'(t_j)| \end{aligned}$$

Here, J_0 is the Bessel function of order 0. Further, (2.8) can be rewritten as

$$u^\infty(\hat{x}) = \frac{e^{-i\pi/4}}{\sqrt{8\pi k}} \int_0^{2\pi} [kv(x(s)) \cdot \hat{x} + \eta] e^{-ik\hat{x} \cdot x(s)} |x'(s)| \varphi(x(s)) ds$$

Then for $n_f \in \mathbb{N}$ with $n_f > 0$ we get the approximation values of the far field pattern at the points $\hat{x}_i = i\pi/n_f$, $i = 0, 1, \dots, n_f$, by the following quadrature rule:

$$u^\infty(\hat{x}_i) \simeq \frac{e^{-i\pi/4}}{\sqrt{8\pi k}} \cdot \frac{\pi}{n} \sum_{j=1, j \neq n}^{2n-1} [kv(x(t_j)) \cdot \hat{x}_i + \eta] e^{-ik\hat{x}_i \cdot x(t_j)} |x'(t_j)| \varphi_j^{(n)}$$

4 The inverse problem

The *inverse problem* we are interested in is, given the far field pattern u^∞ of the scattered wave u^s of the scattering problem (1.1)-(1.3) (or the problem (DP)) for one or a finite number of incident plane waves u^i , to determine the unknown locally rough surface Γ (or the local perturbation Γ_p).

We have the following uniqueness theorem which can be proved by arguing similarly as in the proof of Theorem 3.1 in [21].

Theorem 4.1. Assume that Γ_1 and Γ_2 are two locally rough surfaces and $u_1^\infty(\hat{x}, d)$ and $u_2^\infty(\hat{x}, d)$ are the far field patterns corresponding to Γ_1 and Γ_2 , respectively. If $u_1^\infty(\hat{x}, d_n) = u_2^\infty(\hat{x}, d_n)$ for all $\hat{x} \in S_+$ and $d_n \in S_-$ with $n \in \mathbb{N}$ and a fixed wave number k , then $\Gamma_1 = \Gamma_2$.

Given the incident plane wave $u^i(x) = \exp(ikd \cdot x)$ with the incident direction $d \in S_-$, we define the far field operator F_d mapping the function h_Γ which describes the locally rough surface Γ to the corresponding far field pattern $u_k^\infty(\hat{x}, d)$ in $L^2(S_+)$ of the scattered wave u^s of the scattering problem (1.1)-(1.3):

$$F_d(h_\Gamma) = u_k^\infty(\cdot, d). \quad (4.1)$$

Here, we use the subscript k to indicate the dependence on the wave number k . In terms of this far field operator, given the far-field pattern $u_k^\infty(\hat{x}, d)$, our inverse problem consists in solving the equation (4.1) for the unknown function h_Γ . This is a nonlinear and very ill-posed operator equation. To solving this equation by the Newton method, we need the Frechet differentiability at h_Γ . To this end, let $\Delta h \in C_{0,R}^2(\mathbb{R}) := \{h \in C^2(\mathbb{R}) \mid \text{supp}(h) \subset (-R, R)\}$ be a small perturbation of the function $h_G \in C^2(\mathbb{R})$ and let $\Gamma_{\Delta h} := \{(x_1, h_\Gamma(x_1) + \Delta h(x_1)) \mid x_1 \in \mathbb{R}\}$ denote the corresponding boundary defined by $h_\Gamma(x_1) + \Delta h(x_1)$. Then F_d is called Frechet differentiable at h_Γ if there exists a linear bounded operator $F'_d(h_\Gamma, \cdot) : C_{0,R}^2(\mathbb{R}) \rightarrow L^2(S_+)$ such that

$$\|F_d(h_\Gamma + \Delta h) - F_d(h_\Gamma) - F'_d(h_\Gamma, \Delta h)\|_{L^2(S_+)} = o(\|\Delta h\|_{C^2(\mathbb{R})})$$

as $\|\Delta h\|_{C^2(\mathbb{R})} \rightarrow 0$.

Theorem 4.2. Let $u(x, d) = u^i(x, d) + u^r(x, d) + u^s(x, d)$, where u^s solves the problem (DP) with the boundary data $f = -(u^i + u^r)$. If $h_\Gamma \in C^2$, then F_d is Frechet differentiable at h_Γ and the derivative $F'_d(h_\Gamma, \Delta h) = u'_\infty$ for $\Delta h \in C_{0,R}^2(\mathbb{R})$. Here, u'_∞ is the far field pattern of u' which solves the problem (DP) with the boundary data $f = -(v_2 \Delta h) \partial u / \partial \nu$, where v_2 is the second component of the unit normal ν on Γ directed into the infinite domain D_+ .

Proof. The proof is similar to that of Theorem 4.1 in [4] with appropriate modifications. \square

5 The Newton method with multi-frequency data

We now describe the Newton iteration method for solving our inverse problem of reconstructing the function h_Γ from the far field data, that is, for solving the equation (4.1). Motivated by [4], we use multi-frequency far field data in order to get an accurate reconstruction of the function h_Γ .

For each single frequency data with wave number $k > 0$, we replace (4.1) by the linearized equation

$$F_d(h_\Gamma) + F'_d(h_\Gamma, \Delta h) = u_k^\infty(\cdot, d) \quad (5.1)$$

which we will solve for Δh by using the Levenberg-Marquardt algorithm (see, e.g. [23]) in order to improve an approximation to the function h_Γ . The Newton method consists in iterating this procedure.

In the numerical examples, we consider the noisy measurement data $u_{\delta,k}^\infty(\hat{x}, d_l)$, $\hat{x} \in S_+$, $l = 1, \dots, n_d$, which satisfies

$$\|u_{\delta,k}^\infty(\cdot, d_l) - u_k^\infty(\cdot, d_l)\|_{L^2(S_+)} \leq \delta \|u_k^\infty(\cdot, d_l)\|_{L^2(S_+)}.$$

Here, δ is called a noisy ratio. In practical computations h_Γ has to be taken from a finite-dimensional subspace $R_M \subset C_{0,R}^2(\mathbb{R})$ and the equation (5.1) has to be approximately solved by projecting it on a

finite-dimensional subspace of $L^2(S_+)$ by collocation at a finite number n_f of equidistant points $\hat{x}_j \in S_+$, $j = 1, \dots, n_f$. Let $R_M = \text{span}\{\phi_1, \phi_2, \dots, \phi_M\}$, where $\phi_i, j = 1, 2, \dots, M$, are spline functions with support in $(-R, R)$ (see Remark 5.1 below). Assume that $h^{app} \in R_M$ is an approximation to h_Γ with Γ^{app} being the corresponding boundary. Then, by the strategy in [23], we seek an updated function $\Delta h = \sum_{i=1}^M \Delta a_i \phi_i$ in R_M of h^{app} such that $\Delta a_i, i = 1, \dots, M$, solve the minimization problem:

$$\min_{\Delta a_i} \left\{ \sum_{l=1}^{n_d} \sum_j^{n_f} |F_{d_l}(h^{app})(\hat{x}_j) + F'_{d_l}(h^{app}, \Delta h)(\hat{x}_j) - u_{\delta,k}^\infty(\hat{x}_j, d_l)|^2 + \beta \sum_{i=1}^M |\Delta a_i|^2 \right\} \quad (5.2)$$

where the regularization parameter $\beta > 0$ is chosen such that

$$\begin{aligned} & \left(\sum_{l=1}^{n_d} \sum_j^{n_f} |F_{d_l}(h^{app})(\hat{x}_j) + F'_{d_l}(h^{app}, \Delta h)(\hat{x}_j) - u_{\delta,k}^\infty(\hat{x}_j, d_l)|^2 \right)^{1/2} \\ &= \rho \left(\sum_{l=1}^{n_d} \sum_j^{n_f} |F_{d_l}(h^{app})(\hat{x}_j) - u_{\delta,k}^\infty(\hat{x}_j, d_l)|^2 \right)^{1/2} \end{aligned} \quad (5.3)$$

for a given constant $\rho \in (0, 1)$. Then a new approximation to h_Γ is given as $h^{app} + \Delta h$. Define the error function

$$Err_k = \frac{1}{n_d} \sum_{l=1}^{n_d} \left[\sum_j^{n_f} |F_{d_l}(h^{app})(\hat{x}_j) - u_{\delta,k}^\infty(\hat{x}_j, d_l)|^2 / \sum_j^{n_f} |u_{\delta,k}^\infty(\hat{x}_j, d_l)|^2 \right]^{1/2}$$

Then the iteration is stopped if $Err_k \leq \tau\delta$, where $\tau > 1$ is a fixed constant. See [23] for details.

Remark 5.1. For a positive integer $M \in \mathbb{N}^+$ let $h = 2R/(M + 5)$ and $t_i = (i + 2)h - R$. Then the spline basis functions of R_M are defined by $\phi_i(t) = \phi((t - t_i)/h), i = 1, 2, \dots, M$, where

$$\phi(t) := \sum_{j=0}^{k+1} \frac{(-1)^j}{k!} \binom{k+1}{j} \left(t + \frac{k+1}{2} - j \right)_+^k$$

with $z_+^k = z^k$ for $z \geq 0$ and $= 0$ for $z < 0$. In this paper, we choose $k = 4$, that is, ϕ is the cubic spline function. Note that $\phi_i \in C^3(\mathbb{R})$ with support in $(-R, R)$. See [18] for details.

Remark 5.2. Our inversion Algorithm 5.1 below does not require the locally rough surface Γ to be parameterized by a function h_Γ since, in practical computations, h_Γ is taken from the finite-dimensional subspace R_M spanned by spline functions $\phi_i, j = 1, 2, \dots, M$ with support in $(-R, R)$ (see discussions before Remark 5.1). Therefore, Algorithm 5.1 can deal with more general C^2 -smooth Γ .

Remark 5.3. For the synthetic far-field data of the scattering problem, we choose the coupling parameter $\eta = k$ and get a finite number of measurements $u_{\delta,k}^\infty(\hat{x}_j, d), j = 0, 1, \dots, n_f$, with equidistant points $\hat{x}_j = j\pi/n_f$ for a positive integer $n_f \in \mathbb{N}^+$. For the numerical solution of the scattering problem in each iteration, we choose $\eta = 0$ both to avoid the inverse crime and to reduce the complexity of the computation. Here, we need to assume that k is not a Dirichlet eigenvalue of the region bounded by the curves $\{(x_1, h^{app}(x_1)) \mid x_1 \in [-R, R]\}$ and ∂B_R^- . Further, it is seen from Theorem 4.2 that, in order to compute the Frechet derivative in each iteration we need to compute the normal derivative $\partial u^s / \partial \nu$ of the scattered wave u^s on a subset of $\{x(t_0), x(t_1), \dots, x(t_{2n-1})\}$ which is contained in $\{(x_1, h^{app}(x_1)) \mid x_1 \in$

$(-R, R)$). Since $h^{app} \in C^3(\mathbb{R})$ and the two corners x_A and x_B are not included in the subset, we just use the quadrature rules in [25] in the form (2.2) of the scattered field u^s and the graded mesh with the discrete values $\varphi_j^{(n)}$, $j = 0, 1, \dots, 2n - 1$, of φ which are obtained from the scattering problem in each iteration.

The Newton iteration algorithm with multi-frequency far-field data can be given in the following Algorithm 5.1.

Algorithm 5.1. *Given the far field patterns $u_{\delta, k_i}^\infty(\hat{x}_j, d_l)$, $i = 1, 2, \dots, N$, $j = 0, 1, \dots, n_f$, $l = 1, \dots, n_d$, where $k_1 < k_2 < \dots < k_N$.*

- 1) Let $h^{app} = 0$ be the initial guess of h_Γ and set $i = 0$.
- 2) Set $i = i + 1$. If $i > N$, then stop the iteration; otherwise, set $k = k_i$ and go to Step 3).
- 3) If $Err_k < \tau\delta$, return to Step 2); otherwise, go to Step 4).
- 4) Solve (5.2) with the strategy (5.3) to get an updated function Δh . Let h^{app} be updated by $h^{app} + \Delta h$ and go to Step 3).

Remark 5.4. Our novel integral equation formulation proposed in Section 2 can also be applied to develop a similar Newton inversion algorithm with multiple frequency near-field data.

6 Numerical examples

In this section, several numerical experiments are presented to demonstrate the effectiveness of our algorithm. The following assumptions are made in all numerical experiments.

- 1) For each example we use multi-frequency data with the wave numbers $k = 1, 3, \dots, 2N - 1$, where N is the total number of frequencies.
- 2) To generate the synthetic data and to compute the Frechet derivative in each iteration, we solve the novel integral equation by choosing $n = 128$ for the wave number $k < 13$ and $n = 256$ for the wave number $k \geq 13$.
- 3) We measure the half-aperture (the measurement angle is between 0 and π) far-field pattern with 65 measurement points, that is, $n_f = 64$. The noisy data $u_{\delta, k}^\infty$ are obtained as $u_{\delta, k}^\infty = u_k^\infty + \delta\zeta \|u_k^\infty\|_{L^2(\mathcal{S}_+)} / \|\zeta\|_{L^2(\mathcal{S}_+)}$, where ζ is a random number with $\text{Re}(\zeta), \text{Im}(\zeta) \in N(0, 1)$.
- 4) We set the parameters $\rho = 0.8$ and $\tau = 1.5$.
- 5) In each figure, we use solid line '-' and dashed line '- -' to represent the actual curve and the reconstructed curve, respectively.
- 6) For the shape of the local perturbation of the infinite plane in all examples, we assume that $\text{supp}(h_\Gamma) \in (-1, 1)$; we further choose $R = 1$ and use the smooth curves which are not in R_M .

Example 1. In this example, we consider the case when the local perturbation of the infinite plane is over the x_1 -axis with

$$h_\Gamma(x_1) = \phi((x_1 + 0.2)/0.3),$$

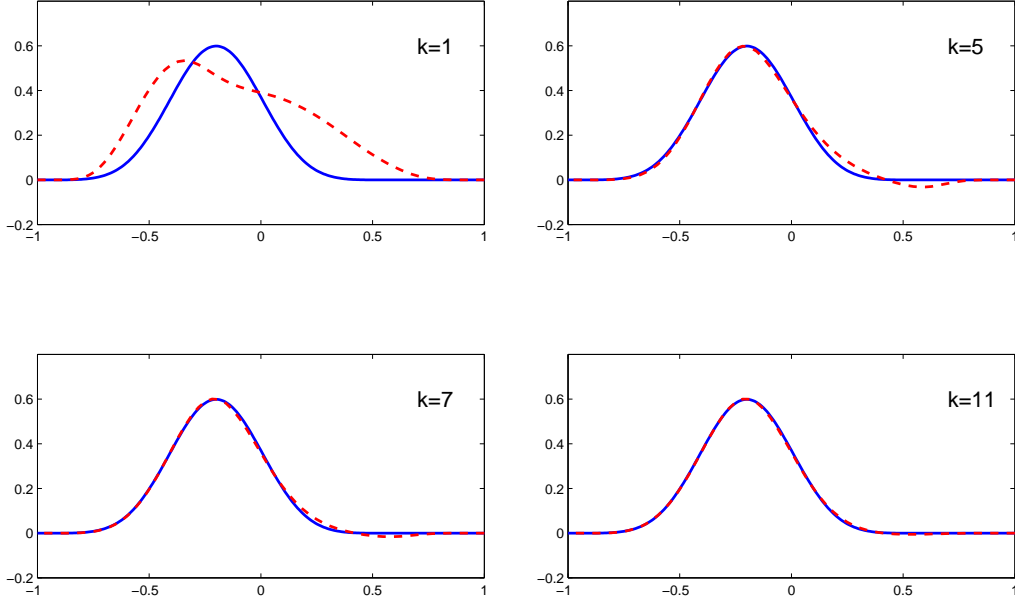


Figure 2: The reconstructed curve (dashed line) at $k = 1, 5, 7, 11$, respectively, from 3% noisy data with one incident direction $d = (\sin(\pi/3), -\cos(\pi/3))$, where the real curve is denoted by the solid line.

where ϕ is defined in Remark 5.1. Here, we consider noisy data with 3% noise and use one incident direction $d = (\sin(\pi/3), -\cos(\pi/3))$. For the inverse problem, we choose the number of the spline basis functions to be $M = 10$ and the total number of frequencies to be $N = 6$. Figure 2 shows the reconstructed curves at $k = 1, 5, 7, 11$, respectively.

Example 2. In this example, we consider the case when the local perturbation of the infinite plane is under the x_1 -axis with

$$h_{\Gamma}(x_1) = -0.8\phi((x_1 - 0.3)/0.2),$$

where ϕ is also given in Remark 5.1. In the inverse problem, the number of the spline basis functions is chosen to be $M = 10$ and the total number of frequencies is chosen to be $N = 9$. Figure 3 presents the reconstructed curves at $k = 1, 5, 11, 17$, respectively, from 3% noisy data with one incident direction $d = (\sin(\pi/3), -\cos(\pi/3))$.

Example 3. The reconstruction considered in this example is a more challenging one with

$$h_{\Gamma}(x_1) = \begin{cases} \exp\left[16/(25x_1^2 - 16)\right] \sin(4\pi x_1), & |x_1| < 4/5 \\ 0, & |x_1| \geq 0 \end{cases}$$

Here, we consider 10% noisy data. In order to get a good reconstruction, the number of the spline basis functions is taken to be $M = 20$ and the total number of frequencies is taken to be $N = 15$. Figure 4 gives the reconstruction at $k = 1, 9, 19, 29$, respectively, with one incident direction $d = (0, -1)$ (normal incidence from the top).

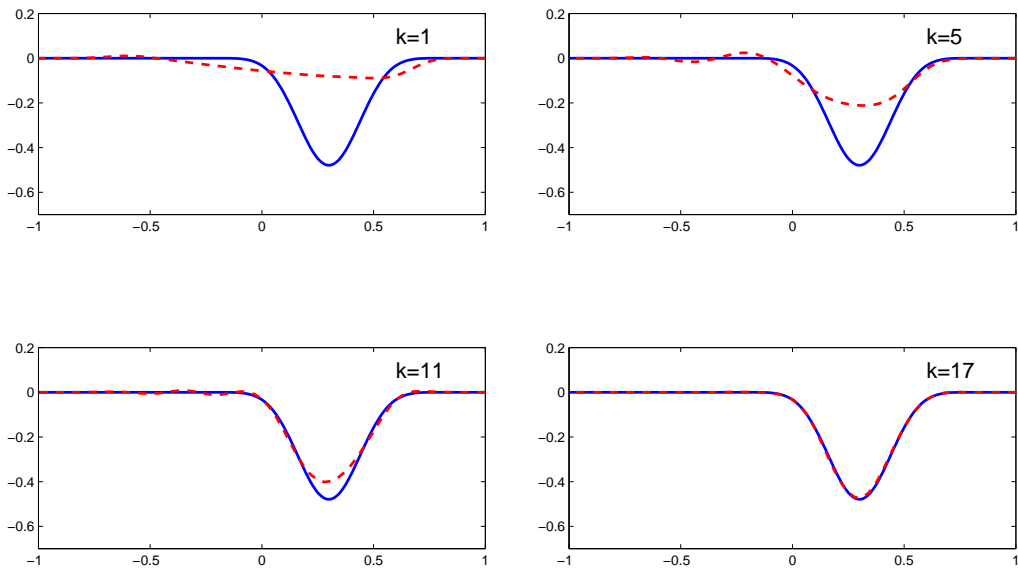


Figure 3: The reconstructed curve (dashed line) at $k = 1, 5, 11, 17$, respectively, from 3% noisy data with one incident direction $d = (\sin(\pi/3), -\cos(\pi/3))$, where the real curve is denoted by the solid line.

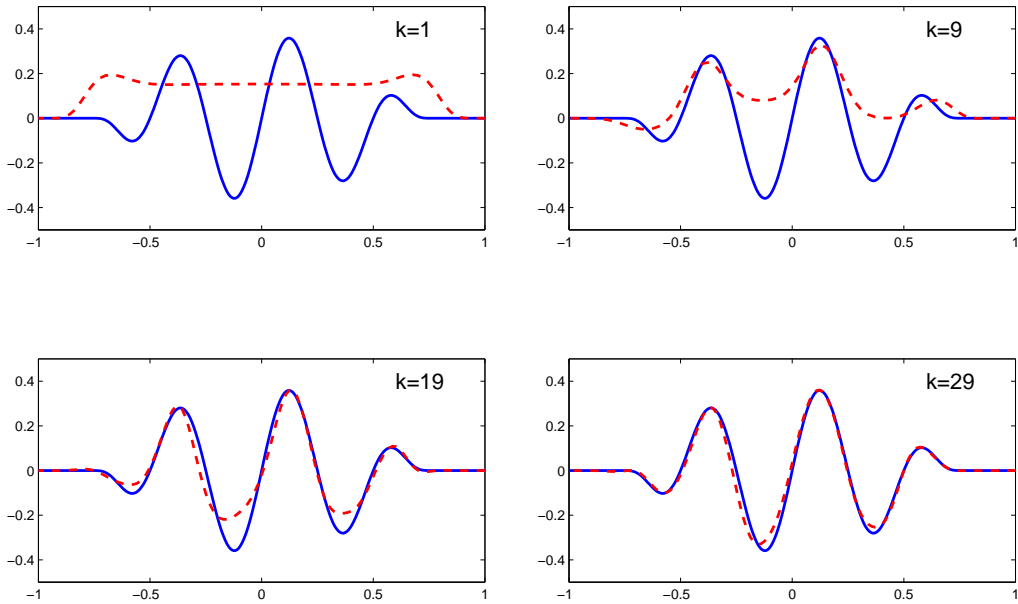


Figure 4: The reconstructed curve (dashed line) at $k = 1, 9, 19, 29$, respectively, from 10% noisy data with normal incidence from the top, where the real curve is denoted by the solid line.

Example 4 (multi-scale profile). We now consider the multi-scale case with

$$h_{\Gamma}(x_1) = \begin{cases} \exp[16/(25x_1^2 - 16)] [0.5 + 0.1 \sin(16\pi x_1)], & |x_1| < 4/5 \\ 0, & |x_1| \geq 0. \end{cases}$$

This function has two scales: the macro-scale is represented by the function $0.5 \exp[16/(25x_1^2 - 16)]$, and the micro-scale is represented by the function $0.1 \exp[16/(25x_1^2 - 16)] \sin(16\pi x_1)$. To capture the two-scale features of the profile, the number of spline basis functions is chosen to be $M = 40$, and the total number of frequencies used is $N = 30$. The reconstruction is obtained with 10% noisy data using one incident plane wave with normal incidence from the top. Figure 5 presents the reconstructed profiles at $k = 9, 33, 45, 59$. From Figure 5 it is observed that the macro-scale features are captured when $k = 9$ (Figure 5, top left), while the micro-scale features are captured at $k = 59$ (Figure 5, bottom right). It is interesting to note that the resolution of the reconstruction does not improve much for $k \in [9, 33]$ and then improves from a larger k (e.g., $k = 45$) until a sufficiently large k (e.g., $k = 59$) for which the whole local rough surface is accurately recovered even with 10% noisy data. This indicates that our Newton algorithm with multiple frequency far-field data can give a stable and accurate reconstruction of multi-scale profiles with noise data as long as sufficiently high frequency data are used. This is similar to the reconstruction algorithm with multi-frequency near-field data developed in [4].

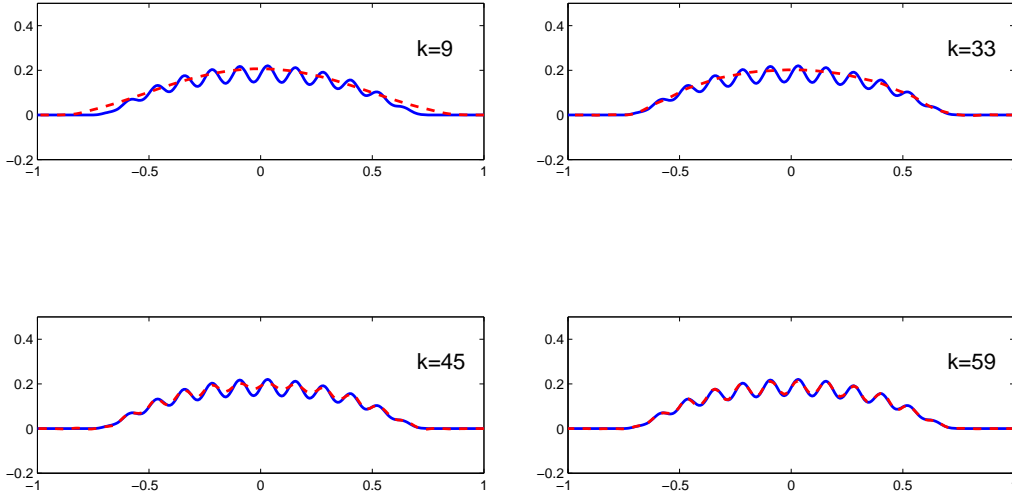


Figure 5: The reconstructed curve (dashed line) at $k = 9, 33, 45, 59$, respectively, from 10% noisy data with normal incidence from the top, where the real curve is denoted by the solid line.

The above numerical results illustrate that the Newton iteration algorithm with multiple frequency data gives a stable and accurate reconstruction of the local perturbation of the infinite plane even in the presence of 10% noise in measurements. From Figures 2-5 it is seen that the upper part of the locally rough surface can be recovered easily at lower frequencies; however, much higher frequencies are needed in order to recover the deep, lower part of the locally rough surface as well as the fine details of the micro-scale features of multi-scale profiles.

We are currently trying to extend the technique to the TM polarization case. Furthermore, it is anticipated that the reconstruction method can be generalized to the three-dimensional case.

Acknowledgements

This work was supported by the NNSF of China under grants 11071244 and 11161130002.

References

- [1] H. Ammari, G. Bao and A. Wood, An integral equation method for the electromagnetic scattering from cavities, *Math. Methods Appl. Sci.* **23** (2000), 1057-1072.
- [2] G. Bao, J. Gao and P. Li, Analysis of direct and inverse cavity scattering problems, *Numer. Math. Theor. Meth. Appl.* **4** (2011), 419-442.
- [3] G. Bao and J. Lin, Near-field imaging of the surface displacement on an infinite ground plane, to appear in *Inverse Problems Imaging*.
- [4] G. Bao and J. Lin, Imaging of local surface displacement on an infinite ground plane: the multiple frequency case, *SIAM J. Appl. Math.* **71** (2011), 1733-1752.
- [5] G. Bao and J. Lin, Imaging of reflective surfaces by near-field optics, *Optics Letters* **37** (2012), 5027-5029.
- [6] G. Bao and W. Sun, A fast algorithm for the electromagnetic scattering from a large cavity, *SIAM J. Sci. Comput.* **27** (2005), 553-574.
- [7] C. Burkard and R. Potthast, A multi-section approach for rough surface reconstruction via the Kirsch–Kress scheme, *Inverse Problems* **26** (2010) 045007 (23pp).
- [8] S.N. Chandler-Wilde and B. Zhang, A uniqueness result for scattering by infinite rough surfaces, *SIAM J. Appl. Math.* **58** (1998), 1774-1790.
- [9] S.N. Chandler-Wilde, C.R. Ross and B. Zhang, Scattering by infinite one-dimensional rough surfaces, *Proc. R. Soc. London A* **455** (1999), 3767-3787.
- [10] S.N. Chandler-Wilde and P. Monk, Existence, uniqueness and variational methods for scattering by unbounded rough surfaces, *SIAM J. Math. Anal.* **37** (2005), 598-618.
- [11] S.N. Chandler-Wilde, E. Heinemeyer and R. Potthast, A well-posed integral equation formulation for three-dimensional rough surface scattering, *Proc. R. Soc. London A* **462** (2006), 3683-3705.
- [12] S.N. Chandler-Wilde, E. Heinemeyer and R. Potthast, Acoustic scattering by mildly rough unbounded surfaces in three dimensions, *SIAM J. Appl. Math.* **66** (2006), 1002-1026.
- [13] S.N. Chandler-Wilde and J. Elschner, Variational approach in weighted Sobolev spaces to scattering by unbounded rough surfaces, *SIAM J. Math. Anal.* **42** (2010), 2554-2580.
- [14] S.N. Chandler-Wilde and C. Lines, A time domain point source method for inverse scattering by rough surfaces, *Computing* **75** (2005), 157-180.

- [15] R. Coifman, M. Goldberg, T. Hrycak, M. Israeli and V. Rokhlin, An improved operator expansion algorithm for direct and inverse scattering computations, *Waves Random Media* **9** (1999), 441-457.
- [16] D. Colton and R. Kress, *Integral Equation Methods in Scattering Theory*, John Wiley, New York, 1983.
- [17] D. Colton and R. Kress, *Inverse Acoustic and Electromagnetic Scattering Theory* (2nd edn), Springer, Berlin, 1998.
- [18] C. de Boor, *A Practical Guide to Splines*, Springer, New York, 2001.
- [19] J.A. DeSanto and R.J. Wombell, Reconstruction of rough surface profiles with the Kirchhoff approximation, *J. Opt. Soc. Amer. A* **8** (1991), 1892-1897.
- [20] J.A. DeSanto and R.J. Wombell, The reconstruction of shallow rough-surface profiles from scattered field data, *Inverse Problems* **7** (1991), L7-L12.
- [21] L. Feng and F. Ma, Uniqueness and local stability for the inverse scattering problem of determining the cavity, *Science China A Math.* **48** (2005), 1113-1123.
- [22] P. Henrici, *Applied and Computational Complex Analysis* Vol. 3, John Wiley, New York, 1986.
- [23] T. Hohage, *Iterative Methods in Inverse Obstacle Scattering: Regularization Theory of Linear and Nonlinear Exponentially Ill-Posed Problems*, PhD thesis, University of Linz, 1999.
- [24] R. Kress, A Nyström method for boundary integral equations in domain with corners, *Numer. Math.* **58** (1990), 145-161.
- [25] R. Kress, On the numerical solution of a hypersingular integral equation in scattering theory, *J. Comp. Appl. Math.* **61** (1995), 345-360.
- [26] R. Kress, *Linear Integral Equations* (2nd edn), Springer, New York, 1999.
- [27] R. Kress and T. Tran, Inverse scattering for a locally perturbed half-plane, *Inverse Problems* **16** (2000), 1541-1559.
- [28] P. Li, An inverse cavity problem for Maxwell's equations, *J. Differential Equations* **252** (2012), 3209-3225.
- [29] C. Ruland, Ein Verfahren zur Lösung von $(\Delta + k^2)u = 0$ Aussengebieten mit Ecken, *Appl. Anal.* **7** (1978), 69-79.
- [30] A. Willers, The Helmholtz equation in disturbed half-spaces, *Math. Methods Appl. Sci.* **9** (1987), 312-323.
- [31] B. Zhang and S.N. Chandler-Wilde, Integral equation methods for scattering by infinite rough surfaces, *Math. Methods Appl. Sci.* **26** (2003), 463-488.